

# A dual probe for selective sensing of Zn (II) by fluorescent and Cu (II) by colorimetric methods in different systems based on 7,8-benzochromone-3-carbaldehyde -(fluorescein)hydrazone

Jie Sun, Tian-rong Li\*, Cong Liu, Jia Xue, Li-mei Tian, Kui Liu, Si-liang Li, Zheng-yin Yang\*

College of Chemistry and Chemical Engineering, State Key Laboratory of Applied Organic Chemistry, Lanzhou University, Lanzhou 730000, PR China

## ARTICLE INFO

### Keywords:

Fluorescent probe  
Benzochromone hydrazone  
Zn<sup>2+</sup>  
Cu<sup>2+</sup>  
Colorimetry

## ABSTRACT

In this study, a novel fluorescent probe sensor, 7,8-benzochromone-3-carbaldehyde (fluorescein)hydrazone L, was designed and synthesized. Based on the photoinduced electron transfer (PET) process, L can detect Zn<sup>2+</sup> in the solution of EtOH/H<sub>2</sub>O (9/1, V/V). The probe had high selectivity and sensitivity to Zn<sup>2+</sup> with a lower detection limit of  $3.4 \times 10^{-7}$  M. Furthermore, the coordination ratio of L-Zn<sup>2+</sup> was 1:1, which could be corroborated by Job's plot. In addition, in the EtOH/ H<sub>2</sub>O (5/2, V/V) solution of the probe L, Cu<sup>2+</sup> was added to produce a marked change in color from achromatous to yellow, indicating that the probe L could detect Cu<sup>2+</sup> by colorimetry, which was detectable by the naked eye, simply and quickly. According to the Benesi-Hildebrand equation, the complexing constants values of L-Zn<sup>2+</sup> and L-Cu<sup>2+</sup> were  $9.8 \times 10^4$  M<sup>-1</sup> and  $1.009 \times 10^5$  M<sup>-1</sup>, respectively.

## 1. Introduction

It is widely known that zinc as a transition metal element ranks second in the human body (second only to iron), and also an essential trace element for animals and plants [1–3]. Zn<sup>2+</sup> plays a vital role in biological activities due to its various coordination methods [4,5]. For example, as one of the auxiliary enzyme components required by many human metabolisms, it regulates the metabolism of the human body, the transmission of neural signals, the transcription and translation of genes, etc [6–10]. At the same time, zinc is a common mineral in the human body. If the content of zinc is insufficient, it would affect children's intellectual development. On the other hand, when the accumulation of Zn<sup>2+</sup> reaches high levels in human body, it can increase the risk of cardiovascular and cerebrovascular diseases [11–16]. In the same way, as the third most abundant transition metal element in the human body, copper is also an indispensable important participant in many life processes [17]. Copper plays a vital role in nerve transmission, oxygen transport, redox, etc [6,18]. However, excessive concentration in cells or tissues of organisms can cause neurodegenerative diseases such as Alzheimer's disease, Monks' disease, Wilson's disease, etc [19–23]. Cu<sup>2+</sup> can also be used to be a cofactor for metalloenzymes and proteins in organisms [24,25]. Hence, maintaining proper levels of copper and zinc

in the body is a key factor in maintaining the health of the body. Due to the widespread use of zinc in the smelting industry, it has caused serious environmental pollution [26]. In a word, it is necessary to design and synthesize a fluorescent chemical sensor to realize the detection of zinc and copper.

The method of fluorescence detection has the advantages of high selectivity, high sensitivity and low detection limit compared with the previous traditional detection methods, such as atomic absorption spectroscopy and atomic emission spectroscopy [27–31]. In view of the above advantages, the method of fluorescence detection is widely applied in ion detection. The fluorescent probe reported in this article has high selectivity and high sensitivity for the detection of metal ions and it is designed and synthesized based on the fluorescence detection method. Herein, the sensor we designed is synthesized by using Schiff base as a raw material. The Schiff base structure provides an electron-rich environment, making it easy to combine with metal ions. Therefore, Schiff base can be regarded as a good ligand [32–34]. In recent years, an increasing number of fluorescent sensors have been exploited to detect metal ions. For instance, Gao et al. compounded a N-(benzimidazol-2-yl) salicylaldehyde (H<sub>2</sub>L) to detect Zn<sup>2+</sup> in dimethyl sulfoxide [1]. Fu et al. synthesized QS to detect Zn<sup>2+</sup> in EtOH/H<sub>2</sub>O (4/1, V/V) [2]. In this article, we report the synthesis of the probe 7,

\* Corresponding authors.

E-mail addresses: [litr@lzu.edu.cn](mailto:litr@lzu.edu.cn) (T.-r. Li), [yangzy@lzu.edu.cn](mailto:yangzy@lzu.edu.cn) (Z.-y. Yang).

<https://doi.org/10.1016/j.jphotochem.2020.113007>

Received 14 September 2020; Received in revised form 24 October 2020; Accepted 27 October 2020

Available online 4 November 2020

1010-6030/© 2020 Elsevier B.V. All rights reserved.

8-benzochromone-3-carbaldehyde-(fluorescein)hydrazone with the fluorescence test of  $\text{Zn}^{2+}$  and the colorimetric test of  $\text{Cu}^{2+}$  in different solvents with this probe. It is necessary to mention that the colorimetric detection of  $\text{Cu}^{2+}$  can be observed with the naked eye which is simple and quick to detect ions [35,36].

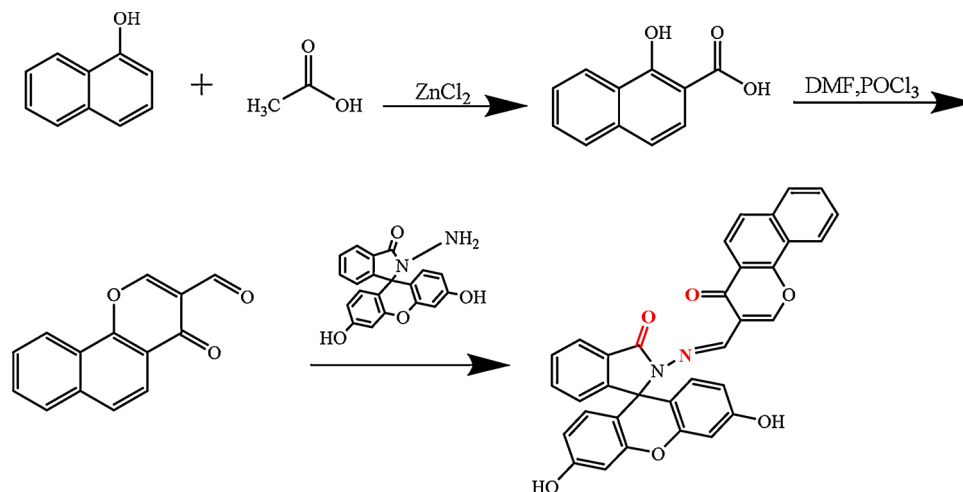
## 2. Experimental

### 2.1. Materials and instruments

All reagents in this experimentation were sourced from commodity suppliers and no further purification was performed when used. Ultra-pure water was used in this experiment. Fluorescence spectrum, UV absorption spectrum, ESI-MS spectrum and  $^1\text{H}$  NMR spectrum were obtained by Hitachi RF-4500 spectrometer equipped with  $1\text{ cm}^{-1}$  quartz cuvette, Shimadzu UV-240 spectrophotometer, Bruker Esquire 600 spectrometer and Bruker 400 MHz with TMS as the internal standard, respectively. The melting point was measured on a Beijing XT4-100x micro-melting point instrument.

### 2.2. Synthesis

4-oxo-4H-benzo[h]methylene-3-carbaldehyde [37] and fluorescein hydrazide [38] were synthesized according to methods reported in previous literature. Based on the following method, 7,8-benzochromone-3-carbaldehyde-(fluorescein)hydrazone (Scheme 1) was synthesized, fluorescein hydrazide (0.24 g, 0.7 mmol) and 4-oxo-4H-benzo[h]methylene-3-carbaldehyde (0.16 g, 0.7 mmol) was dissolved in an appropriate amount of ethanol. The mixture was refluxed for 24 h under stirred condition with appearance of pale yellow precipitate. After that, the mixture was cooled to room temperature and filtered under reduced pressure to obtain a crude product. The obtained crude product was recrystallized from ethanol and then the product was dried in a vacuum to obtain a pale yellow solid. Yield: 72.68 %; mp: 335–338 °C.  $^1\text{H}$  NMR (400 Hz,  $\text{DMSO-d}_6$ , TMS)  $\delta_{\text{H}}$  (ppm): 9.89 (s, 2 H), 8.88 (d, 1H,  $J=0.52$  Hz), 8.44 (q, 1H,  $J=1.76$  Hz), 8.40 (d, 1H,  $J=7.72$  Hz), 8.04 (d, 1H,  $J=7.4$  Hz), 7.90 (m, 3 H), 7.75 (m, 2 H), 7.58 (m, 2 H), 7.07 (m, 1 H), 6.65 (d, 2H,  $J=2.2$  Hz), 6.49 (d, 2H,  $J=8.64$  Hz), 6.43 (dd, 2H,  $J=8.68$  Hz,  $J=2.28$  Hz) (Fig. S1).  $^{13}\text{C}$  NMR (400 Hz,  $\text{DMSO-d}_6$ , TMS)  $\delta_{\text{C}}$  (ppm): 174.74, 164.50, 159.25, 153.29, 153.07, 152.66, 151.45, 140.84, 135.74, 134.79, 130.26, 129.68, 128.87, 128.62, 128.51, 128.22, 126.21, 124.32, 123.90, 123.53, 122.32, 120.38, 120.25, 120.00, 113.03, 110.25, 103.21, 65.65, 56.59, 19.08 (Fig. S3). ESI-MS calculated for  $[\text{M}+\text{H}]^+$  553.1321, found 553.0766.  $[\text{M} + \text{Na}]^+$  575.0566 (Fig. S4).



Scheme 1. Reagents and conditions.

### 2.3. Measurement of UV-vis and fluorescence spectra

Stock solutions ( $5 \times 10^{-3}$  M) of various metal ions ( $\text{Na}^+$ ,  $\text{K}^+$ ,  $\text{Li}^+$ ,  $\text{Ag}^+$ ,  $\text{Ca}^{2+}$ ,  $\text{Ba}^{2+}$ ,  $\text{Mg}^{2+}$ ,  $\text{Zn}^{2+}$ ,  $\text{Cu}^{2+}$ ,  $\text{Hg}^{2+}$ ,  $\text{Pb}^{2+}$ ,  $\text{Mn}^{2+}$ ,  $\text{Ni}^{2+}$ ,  $\text{Co}^{2+}$ ,  $\text{Cd}^{2+}$ ,  $\text{Fe}^{3+}$ ,  $\text{Cr}^{3+}$ ,  $\text{Al}^{3+}$ ) were prepared in ethanol. Stock solution of probe L ( $5 \times 10^{-3}$  M) was obtained in DMF.

In the fluorescence spectroscopy tests, the mixed solution of L (20  $\mu\text{L}$ ) and various metal ions (20  $\mu\text{L}$ ) was added to the cuvette and diluted with EtOH/ $\text{H}_2\text{O}$  solution (9/1, V/V) to 2 mL. For the setting of parameters, the excitation wavelength was set to 428 nm, and the excitation and the emission slit were set to 5 nm and 3 nm, respectively. The detection method of UV-vis spectroscopy was basically the same as that of fluorescence. The only difference was that the diluent of the mixed solution of L (10  $\mu\text{L}$ ) and various metal ions (10  $\mu\text{L}$ ) was EtOH/ $\text{H}_2\text{O}$  solution (5/2, V/V).

## 3. Results and discussion

### 3.1. Effect of solvent

The solvent had a crucial influence on the coordination of the probe L with the metal ion. In order to explore the most suitable solvent for detecting the coordination of L and  $\text{Zn}^{2+}$ , the solvent selection experiment was carried out by the fluorescence spectrum. When the ability of L to recognize various metal ions was studied in ethanol solution, we found that L showed obvious fluorescence upon addition of  $\text{Zn}^{2+}$  or  $\text{Mg}^{2+}$ . Therefore, we tried to distinguish between  $\text{Zn}^{2+}$  and  $\text{Mg}^{2+}$  by changing the solvent.  $\text{Zn}^{2+}$  or  $\text{Mg}^{2+}$  was added into ethanol, methanol, ethyl acetate, DMSO, DMF and acetonitrile solutions respectively to explore the fluorescence emission of probe L. As shown in Fig. 1a, we regretted to find that the fluorescence changes of L on  $\text{Zn}^{2+}$  and L on  $\text{Mg}^{2+}$  were basically the same in the above solvents. Therefore, we chose the ethanol that exhibited the strongest fluorescence after L combining with metal ions as the solvent. And then we tried to add water into ethanol to improve the selectivity of L to metal ions by changing the polarity of the solvent [6]. As described in Fig. 1b, firstly, we tried to add 10 % water to ethanol, namely EtOH/ $\text{H}_2\text{O}$  (10/1, V/V). Although the fluorescence intensity of  $\text{Mg}^{2+}$  decreased significantly, there still showed fluorescence that would interfere with the detection of  $\text{Zn}^{2+}$ . Then, we tried to add 20 % water to ethanol, namely EtOH/ $\text{H}_2\text{O}$  (5/1, V/V). In this solution, the fluorescence of  $\text{Mg}^{2+}$  was almost quenched, but the fluorescence intensity of  $\text{Zn}^{2+}$  was too low. Therefore, we found that the most suitable solvent ratio EtOH/ $\text{H}_2\text{O}$  (9/1, V/V) within the range of 10 %–20 % moisture content.

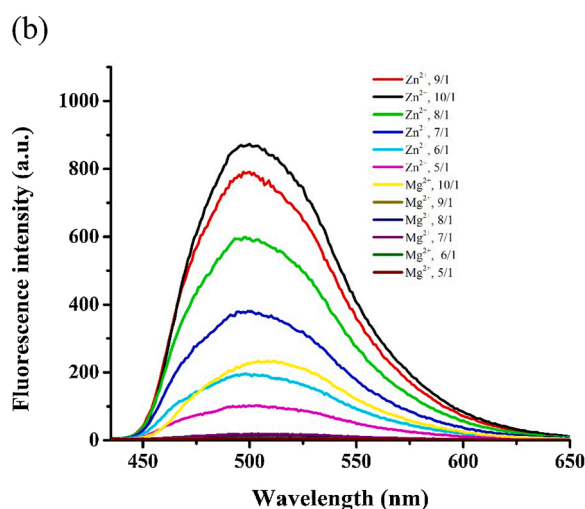
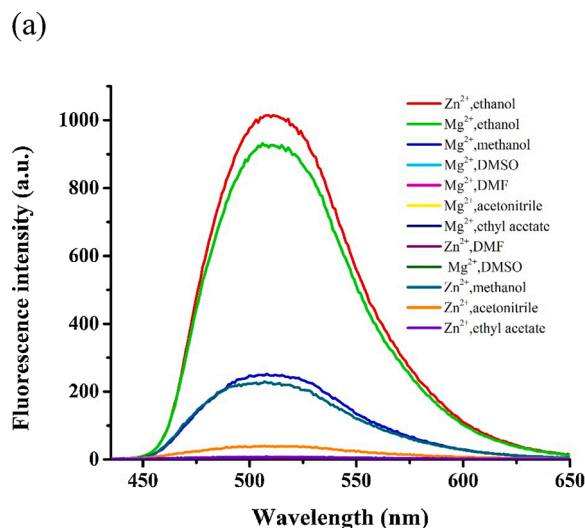


Fig. 1. (a) Solvent effect on fluorescence intensity of the probe L, with  $Zn^{2+}$  in different solvent; (b) Fluorescence spectra of L in EtOH, upon increasing the volume of water percentages from 1/10 to 1/5.

### 3.2. Absorption studies

In EtOH/H<sub>2</sub>O solution (9/1, V/V), the UV–vis titration experiment of L to  $Zn^{2+}$  was carried out at room temperature. The titration spectrum was shown in Fig. 2. In the absence of  $Zn^{2+}$ , the solution of L displayed UV–vis absorption at 280 nm and 325 nm, which might be  $n\text{-}\pi^*$  transitions. And with the continuous addition of  $Zn^{2+}$ , the color of the solution gradually darkened to yellow, the appearance of new absorption bands at 400 nm, 425 nm and 450 nm might be due to  $n\text{-}\pi^*$  transitions [39,40], while the absorption peaks at 280 nm and 325 nm were fallen gradually. And an isotopic site appeared at 364 nm, indicating that L and  $Zn^{2+}$  formed a complex.

### 3.3. Selectivity and competitiveness of L for $Zn^{2+}$

The selectivity of L was analyzed by fluorescence spectroscopy, and the effects of various metal ions on the properties of L were studied. As shown in Fig. 3, under the excitation wavelength of 428 nm, L showed almost no fluorescence emission at 497 nm in EtOH/H<sub>2</sub>O solution (9/1, V/V), after addition of  $Zn^{2+}$ , the significant fluorescence intensity was enhanced. Furthermore, under the same conditions, the solution of L after addition of other different metal ions exhibited hardly any fluorescence emission at 497 nm. The experimental results suggested that, in

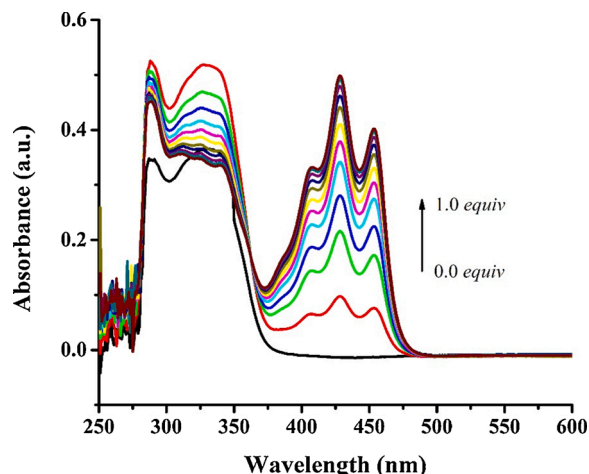


Fig. 2. UV–vis absorption spectra of L (50.0  $\mu$ M) with gradual additional of  $Zn^{2+}$  (0.1–1.0 equiv.) in EtOH/H<sub>2</sub>O (9/1, V/V).

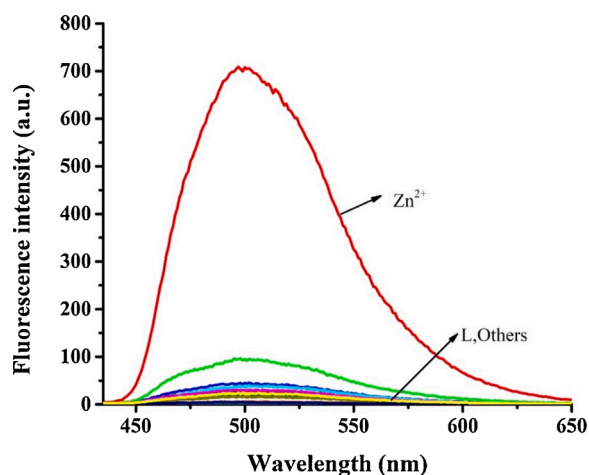


Fig. 3. Fluorescence spectrum of L (50.0  $\mu$ M) in the presence of various metal ion (1.0 equiv.) of  $Ag^+$ ,  $Al^{3+}$ ,  $Ba^{2+}$ ,  $Ca^{2+}$ ,  $Cd^{2+}$ ,  $Co^{2+}$ ,  $Cr^{3+}$ ,  $Cu^{2+}$ ,  $Fe^{3+}$ ,  $Hg^{2+}$ ,  $K^+$ ,  $Li^+$ ,  $Mg^{2+}$ ,  $Mn^{2+}$ ,  $Na^+$ ,  $Ni^{2+}$ ,  $Pb^{2+}$  and  $Zn^{2+}$  in EtOH/H<sub>2</sub>O (9/1, V/V). ( $\lambda_{ex}$  = 428 nm, slit widths: 5 nm/3 nm).

the solution of EtOH/H<sub>2</sub>O (9/1, V/V), L had excellent selectivity for  $Zn^{2+}$ .

In order to further explore the anti-interference ability of L with the addition of  $Zn^{2+}$  in this solution, the fluorescence spectrum was investigated in the presence of other metal ions (1.0 equiv). The results were shown in Fig. 4. When different metal ions were added to the solution of L- $Zn^{2+}$ , most metal ions had little effect on the combination of L- $Zn^{2+}$ . Only the fluorescence emission intensity of  $Cu^{2+}$  at 497 nm was significantly reduced [41]. It might be the magnetic properties of  $Cu^{2+}$  that led to the transfer of electrons and energy from the ligand to the metal ion. In addition, it was worth mentioning that when  $Cu^{2+}$  was added to L, the color of L- $Cu^{2+}$  was also yellow. This result indicated that  $Zn^{2+}$  was more dominant than most other competitive ions in the coordination complex with L.

### 3.4. Selectivity and competitiveness of L for $Cu^{2+}$

To explore the selectivity of the fluorescent probe L towards  $Cu^{2+}$ , the UV–vis absorption spectroscopy experiment of L was conducted in EtOH/H<sub>2</sub>O solution (5/2, V/V) to avoid the interference of  $Zn^{2+}$ . The UV–vis spectrum of L combined with various metal ions was obtained (Fig. 5). The spectrogram displayed that the absorption of L was

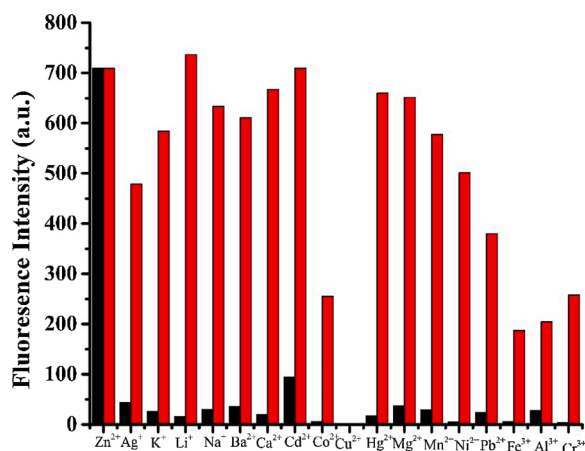


Fig. 4. Fluorescence intensity at 497 nm of L (50.0  $\mu\text{M}$ ) before and after the addition of  $\text{Zn}^{2+}$  (1.0 equiv.) in the presence of various metal ion (1.0 equiv.) of  $\text{Ag}^+$ ,  $\text{Al}^{3+}$ ,  $\text{Ba}^{2+}$ ,  $\text{Ca}^{2+}$ ,  $\text{Cd}^{2+}$ ,  $\text{Co}^{2+}$ ,  $\text{Cr}^{3+}$ ,  $\text{Cu}^{2+}$ ,  $\text{Fe}^{3+}$ ,  $\text{Hg}^{2+}$ ,  $\text{K}^+$ ,  $\text{Li}^+$ ,  $\text{Mg}^{2+}$ ,  $\text{Mn}^{2+}$ ,  $\text{Na}^+$ ,  $\text{Ni}^{2+}$ ,  $\text{Pb}^{2+}$  and  $\text{Zn}^{2+}$  in EtOH/ $\text{H}_2\text{O}$  (9/1, V/V). ( $\lambda_{\text{ex}} = 428$  nm, slit widths: 5 nm/3 nm).

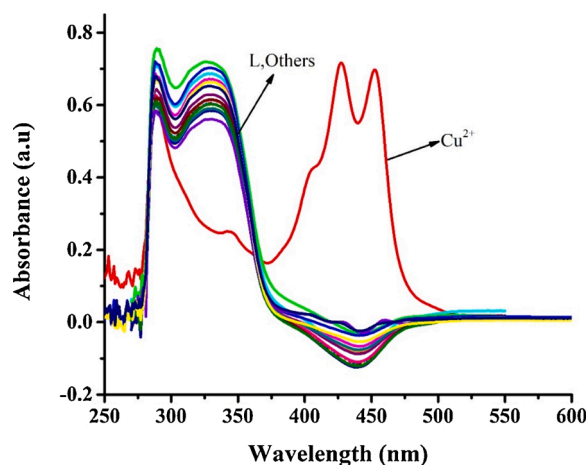


Fig. 5. UV-vis absorption spectra of L (25.0  $\mu\text{M}$ ) in the presence of various metal ion (1.0 equiv.) of  $\text{Ag}^+$ ,  $\text{Al}^{3+}$ ,  $\text{Ba}^{2+}$ ,  $\text{Ca}^{2+}$ ,  $\text{Cd}^{2+}$ ,  $\text{Co}^{2+}$ ,  $\text{Cr}^{3+}$ ,  $\text{Cu}^{2+}$ ,  $\text{Fe}^{3+}$ ,  $\text{Hg}^{2+}$ ,  $\text{K}^+$ ,  $\text{Li}^+$ ,  $\text{Mg}^{2+}$ ,  $\text{Mn}^{2+}$ ,  $\text{Na}^+$ ,  $\text{Ni}^{2+}$ ,  $\text{Pb}^{2+}$  and  $\text{Zn}^{2+}$  in EtOH/ $\text{H}_2\text{O}$  (5/2, V/V).

enhanced obviously at 427 nm and 453 nm after adding  $\text{Cu}^{2+}$  (1.0 equiv.), while L which was added other metal ions showed absorption at 280 nm and 325 nm. To evaluate the competitiveness of  $\text{Cu}^{2+}$ , we continued to add  $\text{Cu}^{2+}$  to the solution of L adding other metal ions. As shown in Fig. 6, the absorbances at 427 nm and 453 nm were increased obviously after the addition of  $\text{Cu}^{2+}$ , at the same time, the absorbances at 280 nm and 325 nm were decreased. This result represented that  $\text{Cu}^{2+}$  had priority over other metals in binding to L.

### 3.5. Binding studies

The Job's plot was used to verify the stoichiometry of L and  $\text{Zn}^{2+}$ . Keeping the total concentration of L and  $\text{Zn}^{2+}$  constant, the molar fraction was  $[\text{L}] / [\text{L} + \text{Zn}^{2+}]$ . As shown in Fig. 7, the fluorescence intensity reached the maximum value at 497 nm when the mole fraction was 0.5. It could be concluded that stoichiometric ratio between L and  $\text{Zn}^{2+}$  was 1:1.

### 3.6. Titration research

In addition, to detect the binding ability between L and the

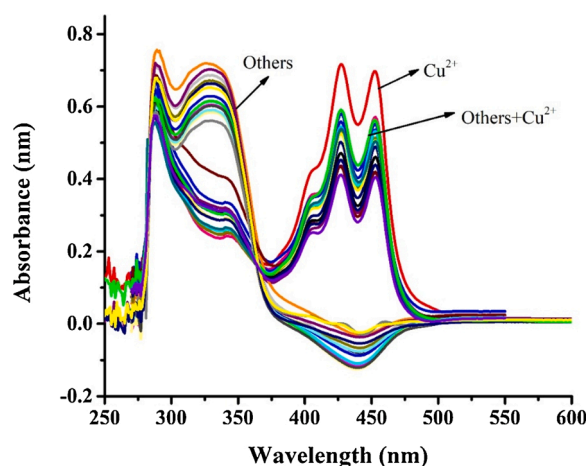


Fig. 6. UV-vis absorption spectra of L (25.0  $\mu\text{M}$ ) before and after the addition of  $\text{Cu}^{2+}$  (1.0 equiv.) in the presence of various metal ion (1.0 equiv.) of  $\text{Ag}^+$ ,  $\text{Al}^{3+}$ ,  $\text{Ba}^{2+}$ ,  $\text{Ca}^{2+}$ ,  $\text{Cd}^{2+}$ ,  $\text{Co}^{2+}$ ,  $\text{Cr}^{3+}$ ,  $\text{Cu}^{2+}$ ,  $\text{Fe}^{3+}$ ,  $\text{Hg}^{2+}$ ,  $\text{K}^+$ ,  $\text{Li}^+$ ,  $\text{Mg}^{2+}$ ,  $\text{Mn}^{2+}$ ,  $\text{Na}^+$ ,  $\text{Ni}^{2+}$ ,  $\text{Pb}^{2+}$  and  $\text{Zn}^{2+}$  in EtOH/ $\text{H}_2\text{O}$  (5/2, V/V).

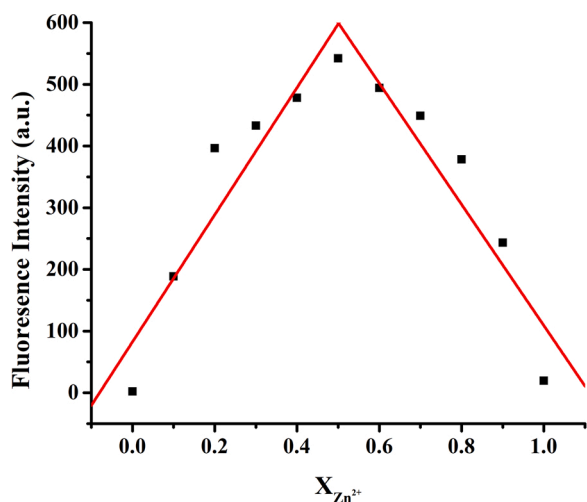


Fig. 7. Job's plot for determining the stoichiometry between L and  $\text{Zn}^{2+}$  in EtOH/ $\text{H}_2\text{O}$  (9/1, V/V). ( $\lambda_{\text{ex}} = 428$  nm, slit widths: 5 nm/3 nm).

concentration of  $\text{Zn}^{2+}$ , a fluorescence titration experiment was conducted. We diluted probe L (5 mM) to 50  $\mu\text{M}$  with a solution of EtOH/ $\text{H}_2\text{O}$  (9/1, V/V), and then dropped  $\text{Zn}^{2+}$  (0.0–1.0 equiv.) continuously to obtain a titration curve (Fig. 8). And in titration, it was so much fun to see that the fluorescence intensity of the probe L had a linear relationship with the concentration of  $\text{Zn}^{2+}$ . The limit of detection (LOD) would be calculated by the formula  $\text{LOD} = 3\sigma / k$  ( $\sigma$ : standard deviation of blank sample,  $k$ : slope of linear relationship curve between fluorescence intensity and  $\text{Zn}^{2+}$  concentration). The detection limit of L to  $\text{Zn}^{2+}$  was calculated to be  $3.369 \times 10^{-7}$  M (Fig. S5). According to the Benesi-Hildebrand formula, the correlation constant is:

$$\frac{1}{F - F_{\min}} = \frac{1}{K_a(F_{\max} - F_{\min})[\text{Zn}^{2+}]} + \frac{1}{F_{\max} - F_{\min}}$$

The meaning of the parameters mentioned in the above formula,  $F_{\max}$ ,  $F$  and  $F_{\min}$  respectively represented the fluorescence intensity at 497 nm in the presence of saturated of  $\text{Zn}^{2+}$ , various concentrations of  $\text{Zn}^{2+}$  and L alone,  $K_a$  was the binding constant of L with  $\text{Zn}^{2+}$ . It was concluded that the complex constant of  $\text{Zn}^{2+}$  with probe L was  $9.8 \times 10^4 \text{ M}^{-1}$  (Fig. S6). In addition, based on the data obtained from the UV-vis spectrum titration experiment of L on  $\text{Zn}^{2+}$ , we calculated the LOD as

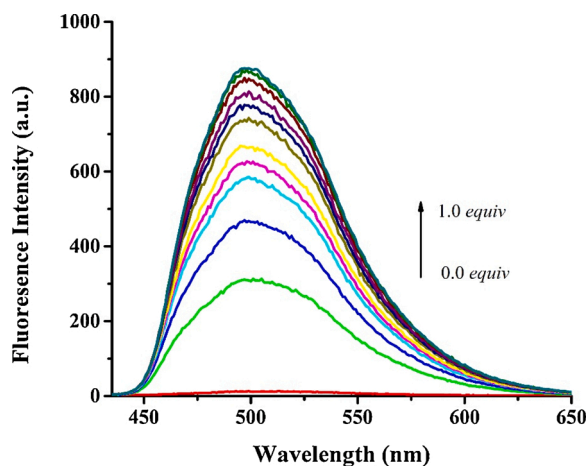


Fig. 8. Fluorescence spectrum of L (50.0  $\mu\text{M}$ ) with gradual titration of  $\text{Zn}^{2+}$  (0–1.0 equiv.) in EtOH/ $\text{H}_2\text{O}$  (9/1, V/V). ( $\lambda_{\text{exc}}$  = 428 nm, slit widths: 5 nm/3 nm).

$2.191 \times 10^{-6}$  M (Fig. S7) and  $K_a$  as  $4.6193 \times 10^4 \text{ M}^{-1}$  (Fig. S8). The results were basically consistent with the results calculated by the fluorescence spectrum titration data.

Similarly, to explore the binding ability between the concentration of L and  $\text{Cu}^{2+}$ , we conducted an ultraviolet titration experiment (Fig. 9). According to the ultraviolet titration spectrum, we linearly fitted the absorbance and the concentration of  $\text{Cu}^{2+}$ . The detection limit (LOD) of the probe L for  $\text{Cu}^{2+}$  was calculated to be  $5.3028 \times 10^{-6}$  M by the formula  $\text{LOD} = 3\sigma / k$  (Fig. S9). In addition, we could linearly fit  $1 / (A - A_{\text{min}})$  and  $1 / [\text{Cu}^{2+}]$  according to the Benesi-Hildebrand equation. It can be concluded that the probe L had a complex constant of  $\text{Cu}^{2+}$  of  $1.009 \times 10^5 \text{ M}^{-1}$  (Fig. S10). In addition, compared with previously reported  $\text{Zn}^{2+}$  and  $\text{Cu}^{2+}$  fluorescent probes, the LOD values given here were basically in the same range (Table 1).

### 3.7. Reaction mechanism of L to $\text{Zn}^{2+}$

The reaction mechanism of L to  $\text{Zn}^{2+}$  seemed to be based on the above-mentioned optical property experiment of L to  $\text{Zn}^{2+}$  and the Job's plot. In the absence of  $\text{Zn}^{2+}$ , the nitrogen atom of the fluorescein hydrazide [42,43] transferred an electron to 4-oxo-4H-benzo[h]methylene-3-carbaldehyde to quench its fluorescence emission. When  $\text{Zn}^{2+}$  was added to L, the coordination of  $\text{Zn}^{2+}$  with the carbonyl oxygen atom of the fluorescein hydrazide part, the oxygen atom of the 4-oxo-4H-benzo[h]methylene-3-carbaldehyde part and the nitrogen atom of  $-\text{C} = \text{N}$  inhibited this electron transfer process and strong fluorescence was emitted, which was based on the photo-induced electron transfer (PET) process [26,44–46]. As a result, intense fluorescence signal was appeared at 497 nm (Scheme 2).

#### 3.7.1. Research on L as a solid probe

In order to detect metal ions more quickly, we designed L as a solid probe. Firstly, the cut filter paper was soaked in the EtOH/ $\text{H}_2\text{O}$  (5:2, V/V) solution of L (50  $\mu\text{M}$ ) and dried it in air. Then, the various metal ion solution ( $\text{Na}^+$ ,  $\text{K}^+$ ,  $\text{Ag}^+$ ,  $\text{Li}^+$ ,  $\text{Mg}^{2+}$ ,  $\text{Zn}^{2+}$ ,  $\text{Ba}^{2+}$ ,  $\text{Cu}^{2+}$ ,  $\text{Mn}^{2+}$ ,  $\text{Ni}^{2+}$ ,  $\text{Cd}^{2+}$ ,  $\text{Co}^{2+}$ ,  $\text{Pb}^{2+}$ ,  $\text{Hg}^{2+}$ ,  $\text{Ca}^{2+}$ ,  $\text{Al}^{3+}$ ,  $\text{Fe}^{3+}$ ,  $\text{Cr}^{3+}$ ) was taken by a clean dropper and dropped it on the filter paper, then  $\text{Cu}^{2+}$  presented a yellow color that was different from other metal ions, which could be observed with the naked eye (Fig. 10). Handled the filter paper immersed in the EtOH/ $\text{H}_2\text{O}$  (9:1, V/V) solution of L in the same way and placed it under a 365 nm UV lamp to observe the difference in luminescence (Fig. 11). Under ultraviolet light,  $\text{Zn}^{2+}$  emitted obvious yellow-green fluorescence. Based on the above experiments, we might be argued that L could be used as a solid probe to detect  $\text{Zn}^{2+}$  and  $\text{Cu}^{2+}$ .

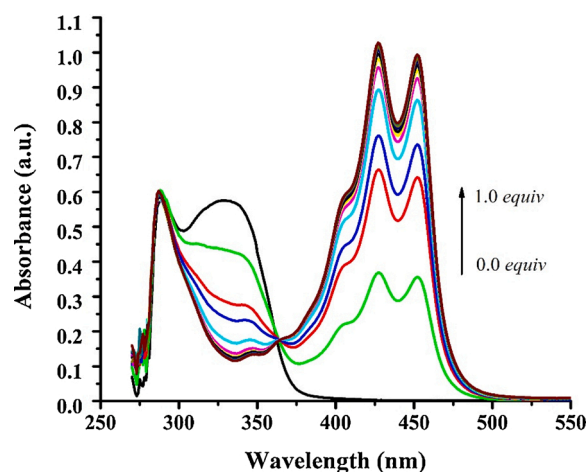


Fig. 9. UV-vis absorption spectra of L (25.0  $\mu\text{M}$ ) with gradual titration of  $\text{Cu}^{2+}$  (0.0–1.0 equiv.) in ethanol/water solution (5/2, V/V).

Table 1

Comparison of probes for  $\text{Zn}^{2+}$ / $\text{Cu}^{2+}$  detection.

Recognition	Solvent (V/V)	LOD/M	Reference
$\text{Zn}^{2+}$	EtOH/ $\text{H}_2\text{O}$ (95/5)	$3.86 \times 10^{-6}$	[32]
$\text{Zn}^{2+}$	$\text{CH}_3\text{CN}/\text{H}_2\text{O}$ (1/1)	$2.92 \times 10^{-7}$	[47]
$\text{Zn}^{2+}$	$\text{CH}_3\text{CN}$	$6 \times 10^{-7}$	[48]
$\text{Zn}^{2+}$	pH = 5.0 MES buffer containing 1 % EtOH	$1.8 \times 10^{-7}$	[49]
$\text{Cu}^{2+}$	HEPES-buffer	$1.6 \times 10^{-7}$	[50]
$\text{Cu}^{2+}$	HEPES-buffer	$1.5 \times 10^{-5}$	[51]
$\text{Cu}^{2+}$	$\text{H}_2\text{O}$	$2.34 \times 10^{-6}$	[52]
$\text{Cu}^{2+}$	HEPES-buffer	$8.9 \times 10^{-8}$	[53]
$\text{Zn}^{2+}$	EtOH/ $\text{H}_2\text{O}$ (9/1)	$3.369 \times 10^{-7}$	This work
$\text{Cu}^{2+}$	EtOH/ $\text{H}_2\text{O}$ (5/2)	$2.191 \times 10^{-6}$	

## 4. Conclusion

In brief, we designed and synthesized a new fluorescent probe L that could detect  $\text{Zn}^{2+}$  and  $\text{Cu}^{2+}$  using fluorescein hydrazide and 4-oxo-4H-benzo[h]methylene-3-carbaldehyde as raw materials. Based on PET mechanism, L could detect  $\text{Zn}^{2+}$  with high selectivity. And the sensitivity of L to  $\text{Zn}^{2+}$  was higher than other ions. The detection limit of L for  $\text{Zn}^{2+}$  was only  $3.369 \times 10^{-7}$  M, which were basically in the same range with the detection limits of the probes previously reported. Moreover, the high sensitivity and high selectivity of L to  $\text{Zn}^{2+}$  was only obtained by the fluorescence method. In addition, adding  $\text{Cu}^{2+}$  to the solution of the probe L in EtOH/ $\text{H}_2\text{O}$  (5/2, V/V) produced a visible color change from colorless to yellow and a change in the ultraviolet-visible spectrum. Similarly, L was more sensitive to  $\text{Cu}^{2+}$  than other metal ions. The above results showed that L could be used as a visual detection probe for  $\text{Cu}^{2+}$  and a fluorescence sensor for  $\text{Zn}^{2+}$ .

### CRedit authorship contribution statement

**Jie Sun:** Conceptualization, Data curation, Formal analysis, Resources, Methodology, Investigation, Software, Validation, Visualization, Writing - original draft, Writing - review & editing. **Tian-rong Li:** Project administration, Supervision. **Cong Liu:** Resources. **Jia Xue:** Resources. **Li-mei Tian:** Resources. **Kui Liu:** Resources. **Si-liang Li:** Resources. **Zheng-yin Yang:** Project administration, Funding acquisition, Supervision.

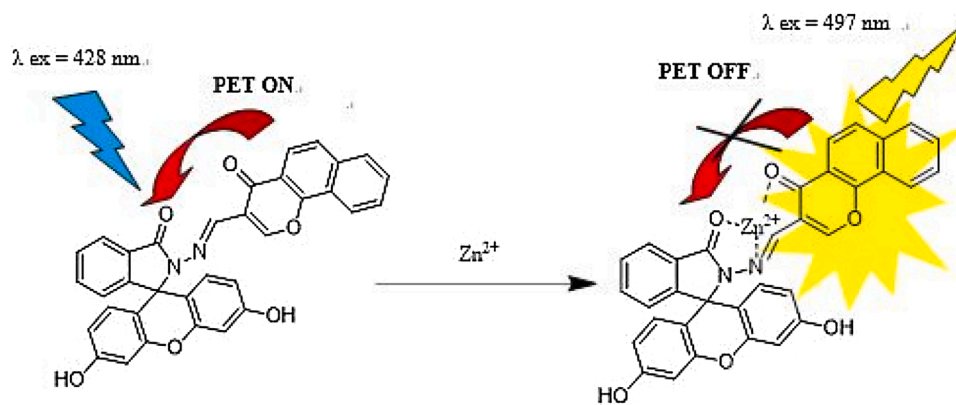
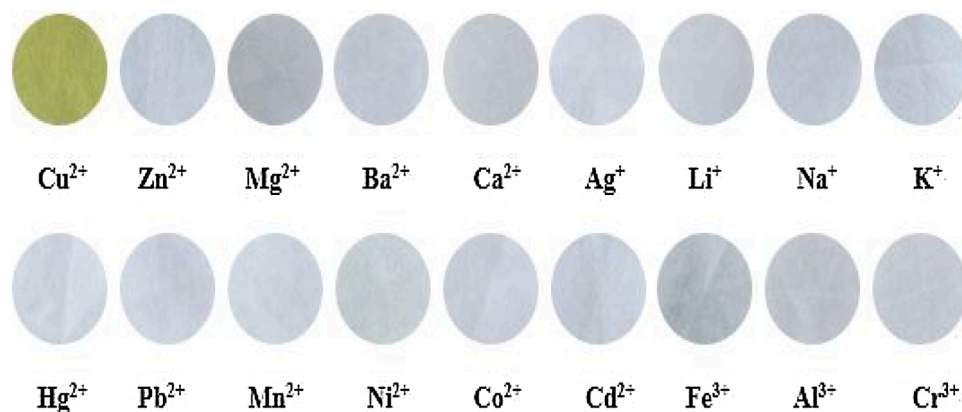
Scheme 2. Reaction mechanism of L on  $Zn^{2+}$ .

Fig. 10. The photograph of filter paper of L after addition of different metal ions under visible light.

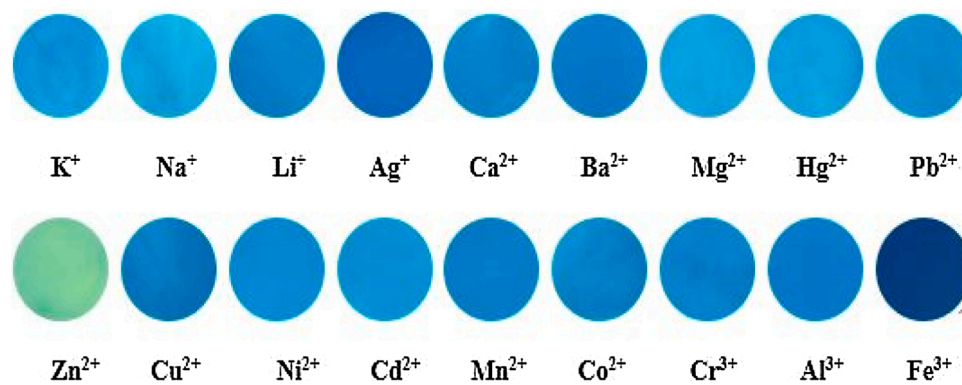


Fig. 11. The photograph of filter paper of L after addition of different metal ions under 365 nm UV lamp.

#### Declaration of Competing Interest

We have no conflicts of interest to declare.

#### Acknowledgment

This work is supported by the National Natural Science Foundation of China (21761019).

#### Appendix A. Supplementary data

Supplementary material related to this article can be found, in the online version, at doi:<https://doi.org/10.1016/j.jphotochem.2020.113007>.

113007.

#### References

- [1] W. Cao, X.J. Zheng, J.P. Sun, W.T. Wong, D.C. Fang, J.X. Zhang, L.P. Jin, *Inorg. Chem.* 53 (2014) 3012–3021.
- [2] J. Fu, Y. Chang, B. Li, H. Mei, K. Xu, *Appl. Organomet. Chem.* 33 (2019).
- [3] M. Taki, J.L. Wolford, T.V. O'Halloran, *J. Am. Chem. Soc.* 126 (2004) 712–713.
- [4] C.J. Frederickson, *Int. Rev. Neurobiol.* 31 (1989) 145–238.
- [5] Y. Li, Z.Y. Yang, Z.C. Liu, B.D. Wang, S.L. Li, *Sens. Actuators B-Chem.* 160 (2011) 1504–1507.
- [6] H.P. Wang, T.T. Kang, X.J. Wang, L.H. Feng, *Talanta* 184 (2018) 7–14.
- [7] J.H. Kim, I.H. Hwang, S.P. Jang, J. Kang, S. Kim, I. Noh, Y. Kim, C. Kim, R. G. Harrison, *Dalton Trans.* 42 (2013) 5500–5507.
- [8] D.S. Auld, *Biometals* 14 (2001) 271–313.
- [9] L. Fan, J.C. Qin, C.R. Li, Z.Y. Yang, *Spectrochim. Acta A.* 236 (2020).

- [10] S. Chakraborty, S. Lohar, K. Dhara, R. Ghosh, S. Dam, E. Zangrando, P. Chattopadhyay, *Dalton Trans.* 49 (2020) 8991–9001.
- [11] V. Bhalla, Roopa, M. Kumar, *Dalton Trans.* 42 (2013) 975–980.
- [12] C.J. Gao, X.J. Jin, X.H. Yan, P. An, Y. Zhang, L.L. Liu, H. Tian, W.S. Liu, X.J. Yao, Y. Tang, *Sens. Actuators B-Chem.* 176 (2013) 775–781.
- [13] J. Xue, L.M. Tian, Z.Y. Yang, *J. Photochem. Photobiol. A: Chem.* 369 (2019) 77–84.
- [14] K.B. Kim, H. Kim, E.J. Song, S. Kim, I. Noh, C. Kim, *Dalton Trans.* 42 (2013) 16569–16577.
- [15] H.G. Lee, J.H. Lee, S.P. Jang, I.H. Hwang, S.-J. Kim, Y. Kim, C. Kim, R.G. Harrison, *Inorg Chim Acta* 394 (2013) 542–551.
- [16] M. Hambidge, *J. Nutr.* 130 (2000) 1344S–1349S.
- [17] Q. Li, Y. Guo, S. Shao, *Sens. Actuators B-Chem.* 171 (2012) 872–877.
- [18] N. D'Ambrosi, L. Rossi, *Neurochem. Int.* 90 (2015) 36–45.
- [19] R. Squitti, *J. Trace Elem. Med. Biol.* 28 (2014) 482–485.
- [20] K.M. Davies, S. Bohic, A. Carmona, R. Ortega, V. Cottam, D.J. Hare, J.P.M. Finberg, S. Reyes, G.M. Halliday, J.F.B. Mercer, K.L. Double, *Neurobiol. Aging* 35 (2014) 858–866.
- [21] S.G. Kaler, *J. Trace Elem. Med. Biol.* 28 (2014) 427–430.
- [22] M. Liggi, M. Sini, O. Sorbello, A. Civolani, L. Demelia, *Clin. Biochem.* 45 (2012) 1095–1096.
- [23] J.L. Yang, X. Xu, S.L. Yang, X.Y. Ji, L.R. Wu, *J. Photochem. Photobiol. A: Chem.* 396 (2020), 112544.
- [24] M. Kujime, H. Fujii, *Tetrahedron Lett.* 46 (2005) 2809–2812.
- [25] C.W. Wu, S.G. Harroun, C.W. Lien, H.T. Chang, B. Unnikrishnan, I.P.J. Lai, J. Y. Chang, C.C. Huang, *Sens. Actuators B-Chem.* 227 (2016) 100–107.
- [26] X. Yuan, X.J. Xu, C.X. Zhao, F. Zhang, Y.X. Lu, Y.J. Shen, C.Y. Wang, *Sens. Actuators B-Chem.* 253 (2017) 1096–1105.
- [27] R. Sangubotla, B.A. Lakshmi, S. Kim, J. Kim, *Appl. Surf. Sci.* 510 (2020), 145417.
- [28] J.S. Wu, W.M. Liu, J.C. Ge, H.Y. Zhang, P.F. Wang, *Chem. Soc. Rev.* 40 (2011) 3483–3495.
- [29] J.J. Du, M.M. Hu, J.L. Fan, X.J. Peng, *Chem. Soc. Rev.* 41 (2012) 4511–4535.
- [30] Z. Zheng, Z.P. Yu, M.D. Yang, F. Jin, Q. Zhang, H.P. Zhou, J.Y. Wu, Y.P. Tian, *J. Org. Chem.* 78 (2013) 3222–3234.
- [31] A. Hazra, A. Roy, A. Mukherjee, G.P. Maiti, P. Roy, *Dalton Trans.* 47 (2018) 13972–13989.
- [32] J.C. Qin, L. Fan, B.D. Wang, Z.Y. Yang, T.R. Li, *Anal. Methods-UK* 7 (2015) 716–722.
- [33] H. Su, L. Hao, W. Hussain, Z.K. Li, H. Li, *CrystEngComm* 22 (2020) 2103–2109.
- [34] F.A. Abebe, C.S. Eribal, G. Ramakrishna, E. Sinn, *Tetrahedron Lett.* 52 (2011) 5554–5558.
- [35] D. Vashisht, S. Sharma, R. Kumar, V. Saini, V. Saini, A. Ibhaddon, S.C. Sahoo, S. Sharma, S.K. Mehta, R. Kataria, *Microchem. J.* 155 (2020), 104705.
- [36] X.L. Xia, D.B. Zhang, C.B. Fan, S.Z. Pu, *Appl. Organomet. Chem.* 34 (2020) e5841.
- [37] M. Jakubek, Z. Kejik, V. Parchansky, R. Kaplanek, L. Vasina, P. Martasek, V. Kral, *Supramol. Chem.* 29 (2017) 1–7.
- [38] T.R. Li, Z.Y. Yang, Y. Li, Z.C. Liu, G.F. Qi, B.D. Wang, *Dye. Pigment.* 88 (2011) 103–108.
- [39] Y.H. Fu, N.S. Finney, *RSC Adv.* 8 (2018) 29051–29061.
- [40] G.R.C. Hamilton, S. Kaur, S. Kamila, B. Callan, J.F. Callan, *New J. Chem.* 42 (2018) 14986–14993.
- [41] H. Seo, M. An, B.-Y. Kim, J.-H. Choi, A. Helal, H.-S. Kim, *Tetrahedron* 73 (2017) 4684–4691.
- [42] F.Y. Yan, K.Q. Fan, Z.J. Bai, R.Q. Zhang, F.L. Zu, J.X. Xu, X. Li, *Trac-Trend Anal. Chem.* 97 (2017) 15–35.
- [43] J. Nebu, J.S.A. Devi, R.S. Aparna, B. Aswathy, G.M. Lekha, G. Sony, *Sens. Actuators B-Chem.* 277 (2018) 271–280.
- [44] W. Sun, M. Li, J.L. Fan, X.J. Peng, *Acc. Chem. Res.* 52 (2019) 2818–2831.
- [45] C.C. Du, S.B. Fu, X.H. Wang, A.C. Sedgwick, W. Zhen, M.J. Li, X.Q. Li, J. Zhou, Z. Wang, H.Y. Wang, J.L. Sessler, *Chem. Sci.* 10 (2019) 5699–5704.
- [46] D. Soni, N. Duvva, D. Badgurjar, T.K. Roy, S. Nimesh, G. Arya, L. Giribabu, R. Chitta, *Chem.-Asian J.* 13 (2018) 1594–1608.
- [47] N.B. Khadke, A.A. Patil, D.Y. Patil, A.V. Borhade, *J. Fluoresc.* 29 (2019) 837–843.
- [48] T.T. Kang, H.P. Wang, X.J. Wang, L.H. Feng, *Microchem. J.* 148 (2019) 442–448.
- [49] H.J. Lee, C.W. Cho, H. Seo, S. Singha, Y.W. Jun, K.H. Lee, Y. Jung, K.T. Kim, S. Park, S.C. Bae, K.H. Ahn, *Chem. Commun.* 52 (2016) 124–127.
- [50] L. Hu, H. Wang, B. Fang, Z.Y. Hu, Q. Zhang, X.H. Tian, H.P. Zhou, J.Y. Wu, Y. P. Tian, *Sens. Actuators B-Chem.* 251 (2017) 993–1000.
- [51] K.S. Lee, J. Park, H.J. Park, Y.K. Chung, S.B. Park, H.J. Kim, I.S. Shin, J.I. Hong, *Sens. Actuators B-Chem.* 237 (2016) 256–261.
- [52] R. Boroujerdi, *J. Fluoresc.* 26 (2016) 781–790.
- [53] S.W. Cho, A.S. Rao, S. Bhunia, Y.J. Reo, S. Singha, K.H. Ahn, *Sens. Actuators B-Chem.* 279 (2019) 204–212.